Accepted Manuscript

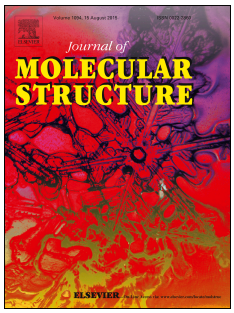

Synthesis, characterization, computational studies, antimicrobial activities and carbonic anhydrase inhibitor effects of 2-hydroxy acetophenone-*N*-methyl *p*-toluenesulfonylhydrazone and its Co(II), Pd(II), Pt(II) complexes

Neslihan Özbek, Saliha Alyar, Burcu Koçak Memmi, Ayla Balaban Gündüzalp, Zafer Bahçeci, Hamit Alyar

PII: S0022-2860(16)30816-X

DOI: 10.1016/j.molstruc.2016.07.122

Reference: MOLSTR 22825

To appear in: *Journal of Molecular Structure*

Received Date: 19 March 2016

Revised Date: 28 July 2016

Accepted Date: 31 July 2016

Please cite this article as: N. Özbek, S. Alyar, B.K. Memmi, A.B. Gündüzalp, Z. Bahçeci, H. Alyar, Synthesis, characterization, computational studies, antimicrobial activities and carbonic anhydrase inhibitor effects of 2-hydroxy acetophenone-*N*-methyl *p*-toluenesulfonylhydrazone and its Co(II), Pd(II), Pt(II) complexes, *Journal of Molecular Structure* (2016), doi: 10.1016/j.molstruc.2016.07.122.

2-Hydroxyacetophenone-N-methyl p-toluenesulfonylhydrazone *(afptsmh)* and its Co(II), Pd(II) and Pt(II) metal complexes were synthesized for the first time and investigated their antibacterial activities and carbonic anhydrase enzyme inhibitor effects. Also ^{1}H and ^{13}C shielding tensors for crystal structure were calculated with GIAO/DFT/B3LYP/6-311++G(d,p) methods in $CDCl_3$.

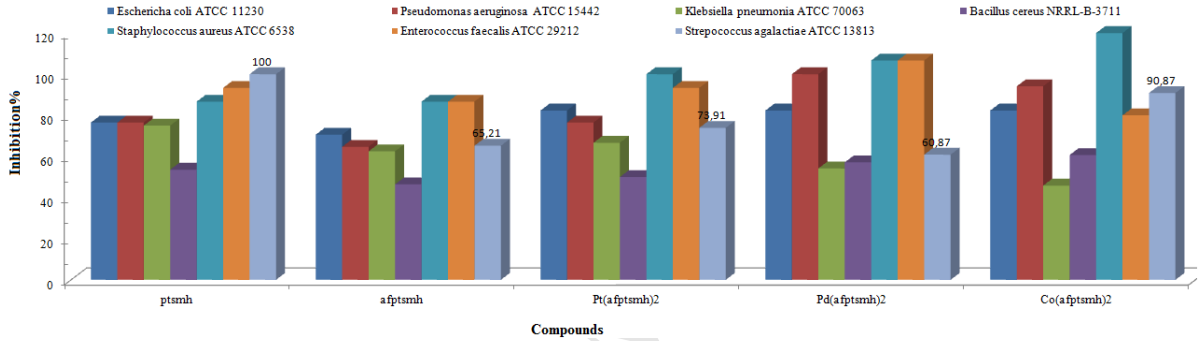

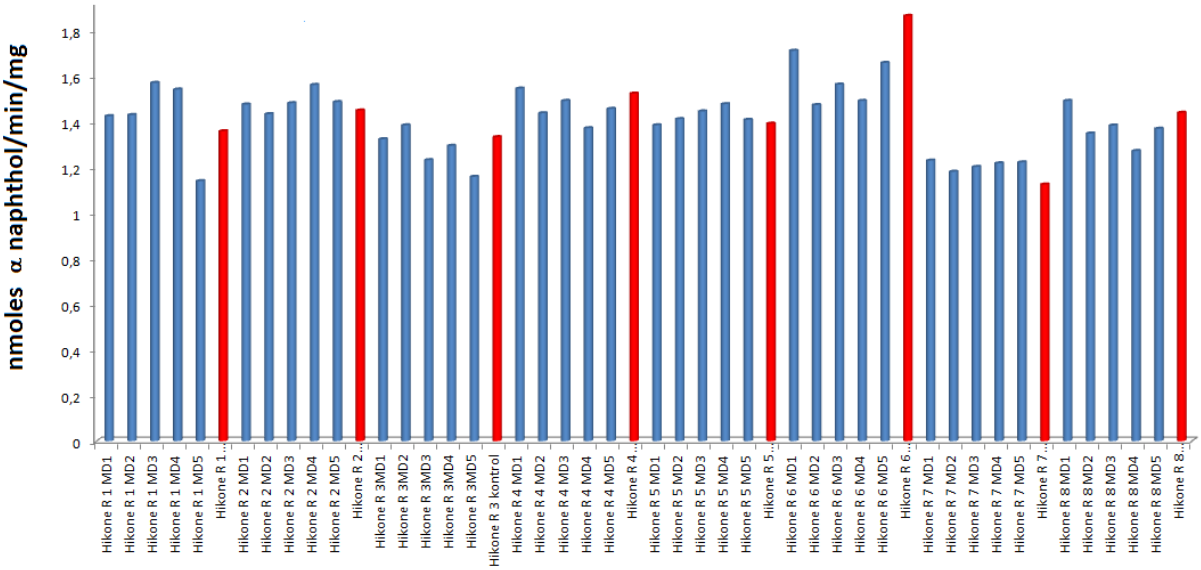

Synthesis, characterization, computational studies, antimicrobial activities and carbonic anhydrase inhibitor effects of 2-hydroxy acetophenone-N-methyl *p*-toluenesulfonylhydrazone and its Co(II), Pd(II), Pt(II) complexes

Neslihan Özbek[1]✉, Saliha Alyar[2], Burcu Koçak Memmi[3], Ayla Balaban Gündüzalp[4], Zafer Bahçeci [1], Hamit Alyar[5]

✉ Neslihan Özbek*: ege_nesliozbek@hotmail.com*

[1]*Department of Primary Education, Faculty of Education, Ahi Evran University, 40100 Kırşehir, Turkey*

[2]*Department of Chemistry, Science Faculty, Karatekin University, 18100 Çankırı, Turkey*

[3] *Insecticide Test Laboratory, Hacettepe University, 06800 Ankara, Turkey*

[4]*Department of Chemistry, Science Faculty, Gazi University, 06500, Ankara, Turkey*

[5]*Department of Physics, Science Faculty, Karatekin University, 18100 Çankırı, Turkey*

ABSTRACT

2-Hydroxyacetophenone-N-methyl *p*-toluenesulfonylhydrazone (*afptsmh)* derived from *p*-toluenesulfonicacid-1-methylhydrazide *(ptsmh)* and its Co(II), Pd(II), Pt(II) complexes were synthesized for the first time. Synthesized compounds were characterized by spectroscopic methods (FT-IR, ^{1}H-^{13}C NMR, LC-MS, UV-vis), magnetic susceptibility and conductivity measurements. ^{1}H and ^{13}C shielding tensors for crystal structure of ligand were calculated with GIAO/DFT/B3LYP/6-311++G(d,p) methods in $CDCl_3$. The vibrational band assignments were performed at B3LYP/6-311++G(d,p) theory level combined with scaled

quantum mechanics force field (SQMFF) methodology. The antibacterial activities of synthesized compounds were studied against some Gram positive and Gram negative bacteria by using microdilution and disc diffusion methods. In vitro enzyme inhibitory effects of the compounds were measured by UV–vis spectrophotometer. The enzyme activities against human carbonic anhydrase II (hCA II) were evaluated as IC_{50} (the half maximal inhibitory concentration) values. It was found that *afptsmh* and its metal complexes have inhibitory effects on hCA II isoenzyme. General esterase activities were determined using alpha and beta naphtyl acetate substrates (α- and β-NAs) of *Drosophila melanogaster (D. melanogaster).* Activity results show that afptsmh does not strongly affect the bacteria strains and also shows poor inhibitory activity against hCAII isoenzyme whereas all complexes posses higher biological activities.

Keywords: Sulfonamides, B3LYP, disc diffusion method, MICs, hCA II, *D. melanogaster*

1. Introduction

Sulfonamides have been intensively investigated as the first effective antibacterial [1,2] and chemotherapeutic agents employed systematically for the prevention and the cure of bacterial infections in humans and other animal systems [3,4]. Sulfamethoxazole with trimethoprim (SMX/TMP) is a drug combination with broad-spectrum of antibacterial activities against both Gram positive and Gram negative organisms. SMX/TMP is currently the most effective therapeutic agent against *P.J. pneumonia* in patients with AIDS [5]. Later on, many thousands of molecules containing sulfanilamide group have been created yielding formulations with greater effectiveness and less toxicity. Sulfa drugs are still widely used for conditions such as acne and urinary tract infections and they have great interest for the

treatment of infections having bacterial resistant to other antibiotics. Also, the other activities include endotelin antagonism, anti-inflammatory activity, tubular transport inhibition, insulin release, carbonic anhydrase and saluretic actions [8]. Some metal sulfonamides have been attracted much attention due to higher activities than free ligands and the corresponding metallic salts. In particular, Ag-sulfadiazine has been proved to be an effective topical antimicrobial agent having significance in burn therapy with better activities than free ligand or $AgNO_3$ [9]. Moreover, several Cu(II), Ce(III), Bi(III), Cd(II) and Hg(II) sulfonamide complexes were evaluated for their antibacterial activities [10-12]. One of the most important activity of the sulfonamides is the enzyme inhibition effect to zinc containing metalloenzyme named as carbonic anhydrase (CA). Many sulfonamide CA inhibitors have been used as antiglaucoma, diuretic, antiobesity and antitumor agents and various neurological disorders [13-15].

In our previous studies, aliphatic/aromatic bis sulfonamides were synthesized and tested for antimicrobial activities [16-29]. Also, we have reported conformational analysis and vibrational spectroscopic investigation of the methanesulfonic acid hydrazide, [20] methanesulfonic acid 1-methylhydrazide [21] and some methanesulfonylhydrazone derivatives [22,23]. In this work, 2-hydroxyacetophenone-N-methyl *p*-toluenesulfonylhydrazone (*afptsmh*) derived from *p*-toluenesulfonicacid-1-methylhydrazide *(ptsmh)* and its Co(II), Pd(II), Pt(II) complexes were synthesized and characterized by using elemental analyses, spectrometric methods (FT-IR, ^{1}H-^{13}C NMR, LC–MS, UV-vis), magnetic susceptibility and conductivity measurements. ^{1}H and ^{13}C shielding tensors for crystal structure of ligand were calculated with GIAO/DFT/B3LYP/6-311++G(d,p) methods in $CDCl_3$. The vibrational band assignments were performed at B3LYP/6-311++G(d,p) theory level combined with scaled quantum mechanics force field (SQMFF) methodology. The antibacterial activities of compounds were studied against Gram positive species; *B.subtilis*

ATCC 6633, *B. cereus* NRRL-B-3711, *S. aureus* ATCC 6538, *E. faecalis* ATCC 29212, *S. agalactiae* ATCC 13813 and Gram negative species; *E. coli* ATCC 11230, *P. aeruginosa* ATCC 15442, *K. pneumonia* ATCC 70063 by using microdilution (as MICs) and disc diffusion (as mm zone) methods. The inhibition degrees of the compounds on carbonic anhydrase II (hCA II) have been evaluated as IC_{50} (the half maximal inhibitory concentration) and we also report the α esterase activities and the β- esterase activities from the model of insect *D. melanogaster*.

2. Experimental

2.1. Instrumentation

The elemental analyses (C, H, N and S) were performed on a LECO CHNS 9320 type elemental analyzer. The IR spectra (4000-400 cm^{-1}) were recorded on a Mattson 1000 FT-IR Spectrophotometer with samples prepared as KBr pellets. LC/MS-APCI was recorded on an AGILENT 1100 Spectrometer. The melting points were measured using an Opti Melt apparatus. TLC was conducted on 0.25 mm silica gel plates (60F $_{254}$, Merck). The molar magnetic susceptibilities were measured on powdered samples using Gouy method. The molar conductance measurements were carried out using a Siemens WPA CM 35 conductometer. All solvents were purchased from Merck and reagents were obtained from Aldrich Chem. Co. (ACS grade) and used as received. The microdilution broth method was used to determine antibacterial activities of the compounds against Gram positive species; *B. subtilis* ATCC 6633, *B. cereus* NRRL-B-3711, *S. aureus* ATCC 6538, *E. faecalis* ATCC 29212, *S. agalactiae* ATCC 13813 and Gram negative species; *E. coli* ATCC 11230, *P. aeruginosa* ATCC 15442, *K. pneumonia* ATCC 70063. The enzyme activity measurements were also performed by using microplate reader (Biotek spectrophotometer, Vermont, USA).

2.2. Synthesis

p-Toluenesulfonic acid 1-methylhydrazide(ptsmh)

p-Toluenesulfonyl chloride (0.04 mol, 7.626 g) in tetrahydrofuran (30 mL) was added dropwise to solution of methylhydrazine (0.05 mol, 1.60 mL) in ethanol/ethyl acetate (1:1) while the temperature was maintained between 268-273 K. The mixture was stirred for 24 h mean while the completion of the reaction was monitored by TLC and then, the solvent was evaporated. The colorless crude compound was purified in THF/n-hexane (1:1) by column chromatography and then the product was recrystallized from THF/n-hexane mixture (1:1) [24]. Yield 72%; mp: 115–117^{0}C. Elemental analysis results for $C_8H_{12}N_2O_2S$: (Calc.%) C, 47.98; H, 6.04; N, 13.99; S, 16.01. (Found%): C, 45.55; H, 6.20; N, 14.25; S, 17.10. LC-MS: m/z (abudance %) $[M+1]^+$:200.15 (54%), $[M-N(CH_3)-NH_2]^+$:155.85 (100%).

2-Hydroxyacetophenone-N-methyl p-toluenesulfonylhydrazone (afptsmh)

p-Toluenesulfonic acid 1-methylhydrazide (1.5 g, 4.72 mmol) in ethanol/ethyl acetate (1:1) solution was added dropwise to solution of 2'-hydroxyacetophenone (0.52 g, 5.0 mmol) in ethanol/ethyl acetate (1:1) maintaining the temperature at about 323 K. Then, the mixture was stirred for 24 h at room temperature. The precipitated product was recrystallized from ethanol/n-hexane (2:1) mixture. The yellow crystalline solid was dried in vacuo to remove ethanol/n-hexane vapour. Yield 65%. Mp. 155-157 ^{0}C. Elemental analysis for $C_{16}H_{18}N_2O_3S$ (Calc.%) C 60.36, H 5.70, N 8.80, S 10.07. (Found%) C 59.80, H 5.74, N 9.20, S 10.22. LC-MS: m/z (abudance %) 319.8 $[M+2]^+$:319.8 (25.5%), $[M-AfOH]^+$: 198.6 (100%).

Synthesis of the complexes

All metal complexes were prepared by the following general method: To solution of *afptsmh* (2.0 mmol) in acetonitrile (2.0 mL), anhydrous 0.80 mmol MCl_2 (where M: Pt(II), Pd(II) and

Co(II)) dissolved in methanol/acetonitrile (2:1, 30 mL) was added and then, NaOH in methanol (2 mL) was added to obtain alkaline media. The reaction mixture was heated at 60 ^{0}C for one hour by stirring on magnetic stirrer. The metal complexes were precipitated at room temperature and filtered off, dried in a desiccator over $CaCl_2$.

Trans-bis(2-Hydroxyacetophenone-N-methyl p-toluenesulfonylhydrazonato)platinum(II) (*Pt(afptsmh)$_2$*) Yield 85%. Mp. 317-319 ^{0}C. Elementel analysis for $C_{32}H_{34}N_4O_6S_2Pt$ (Calc.%) C 46.32, H 4.13, N 6.75, S 7.73, Pt 23.51. (Found%) C 48.10, H 3.80, N 6.95, S 7.24, Pt 23.48. APCL-MS: m/z (abudance %) $[M+1]^+$: 830.2 (14.8%).

Trans-bis(2-Hydroxyacetophenone-N-methyl p-toluenesulfonylhydrazonato)palladium(II) (*Pd(afptsmh)$_2$*) Yield 70%. Mp. 287-289 ^{0}C. Elemental analysis for $C_{32}H_{34}N_4O_6S_2Pd$ (Calc.%) C 51.86, H 4.62, N 7.56, S 8.65, Pd 14.36 (Found%) C 50.16, H 4.45, N 7.14, S 8.85, Pd 14.28. APCL-MS m/z (abudance%) $[M+1]^+$: 741.8 (19.9%)

Trans-bis(2-Hydroxyacetophenone-N-methyl p-toluenesulfonylhydrazonato)cobalt(II) (*Co(afptsmh)$_2$*) Yield 80%. Mp. 284-286 ^{0}C. μ_{eff}:3.89 BM. Elemental analysis for $C_{32}H_{34}N_4O_6S_2Co$ (Calc.%) C 55.40, H 4.94, N 8.08, S 9.24, Co 8.50. (Found%) C 55.31, H 4.55, N 8.22, S 8.95, Co 8.45. APCL-MS m/z (abudance%) $[M+1]^+$: 694.1(12.6%).

2.3. Computational Details

The molecular geometry optimizations, frontier molecular orbital (HOMO and LUMO) energies and vibration frequency calculations for *afptsmh* were performed with Gaussian 03W software package by using DFT approaches [25]. The split valence 6-311++G (d, p) basis set was used for the expansion of the molecular orbitals [26]. The geometries were fully optimized (as seen in Fig.1a) without any constraint with the help of analytical gradient procedure implemented within Gaussian 03W program. All the parameters were allowed to

relax and all the calculations were converged for optimized geometry which corresponds to true energy minimum as revealed by the lack of imaginary values in the wave number calculations. The vibrational band assignments were performed at B3LYP/6-311++G (d,p) theory level combined with scaled quantum mechanics force field (SQMFF) methodology. The ^{1}H and ^{13}C NMR chemical shifts of the compounds were calculated in $CDCl_3$ using the GIAO method. Also, HOMO and LUMO energies of the compounds were calculated using DFT procedure with the B3LYP/LanL2DZ level. The structure sketches of the complexes were presented at Fig. 1b.

2.4. Procedure for Antibacterial Activity

Microdilution assay

The minimal inhibition concentration (MIC) is defined as the lowest concentration of the compounds to inhibit the growth of the microorganisms. The inocula of microorganisms were prepared from 12 h broth cultures and suspensions were adjusted to 0.5 McFarland standard turbidity. The tested compounds dissolved in 20% DMSO were first diluted to the highest concentration (2000 μg mL^{-1}) and then serial two-fold dilutions were applied at the concentration range from 15.625 to 2000 μg mL^{-1} in 10 mL sterile test tubes containing nutrient broth. The MIC value of each compound against bacterial strain was determined based on a microdilution method [27]. The 96-well plates were prepared by dispensing 95 μL of nutrient broth and 5 μL of the inoculums into each well. 100 μL from each of the test compounds initially prepared at the concentration of 2400 μg mL^{-1} was added into the first well in the plate. Then, 100 μL from each of serial dilutions was added to eight consecutive wells. The last well containing 195 μL of nutrient broth without compound and 5 μL of inoculum was used as negative control. The contents of the wells were mixed and the micro

plates were incubated at 37 ^{0}C for 24 h. All compounds tested in this study were screened twice against each microorganism.

Disc diffusion method

The synthesized ligand and its complexes were dissolved in dimethylsulfoxide (20% DMSO) to final concentration of 10 mg mL^{-1} and sterilized by filtration through 0.45 µm millipore filters. Antimicrobial activity tests were then carried out by disc diffusion method using 100 µL of suspension containing 10^{8} CFU mL^{-1} bacterial spread on a nutrient agar (NA) medium. The discs (6 mm in diameter) were impregnated with 20 µL of each compound (200 µg/disc) at the concentration of 10 mg mL^{-1} and placed on the inoculated agar. The discs impregnated with 20% DMSO were used as negative control. Sulfamethoxazole (*SD1*, 300 µg/disc), sulfioxazole (*SD2*, 300 µg/disc) were used as positive controls (standard drugs) to determine the sensitivity of one strain/isolate in each microbial species. The inoculated plates were incubated at 37 ^{0}C for 24 h for bacterial strain isolates. Antimicrobial activities in the disc diffusion assay were evaluated by measuring mm zone of inhibition against tested microorganisms. Each assay in this study was repeated twice [28, 29].

2.5. Procedure for hCA II inhibition

The organism and environmental conditions

Hikone-R marker stock collected from minimum 40 *D. melanogaster* culture was obtained from Bloomington Stock Center. The flies were kept in *D. melanogaster* culture room (Hacettepe University, Ankara/Turkey) at 25±1^{0}C and relative humidity of 50-60% and in 12h light, 12 h dark periods on a standard Carolina *D. melanogaster* medium.

General esterase activity assay for D. melanogaster

General esterase experiments were adapted to *D. melanogaster* from the World Health Organization (WHO) manual for the determination of insecticide resistance mechanisms. Activity measurements were done only on male individuals collected from egg and kept at -80 ^{0}C [30]. Briefly, *D. melanogaster* samples were taken from the freezer, daily and one individual was placed into each eppendorf tube and homogenized with the addition of 200 mL homogenization buffer (50 mM sodium phosphate buffer, pH 7.5 containing 1% triton X-100). The homogenate was centrifuged for 10 minutes at 14000 rpm at 4^{0}C in a refrigerated centrifuge. The supernatant was taken with micropipette and placed in a 96–well microplate and used as the enzyme source. α- and β- naphtyl acetates (α- and β-NAs) were used as substrates. Reaction was stopped by adding fast blue B-SDS solution and absorbance was determined at 600 nm for α-NA and at 560 nm for β-NA.

The antibacterial activity experiments were performed for 5 different compounds (*ptsmh MD1, afptsmh MD2,* Pd(a*fptsmh*)$_2$ MD3, Pt(a*fptsmh*)$_2$ MD4, Co(a*fptsmh*)$_2$ MD5) and positive controls.

Protein assay

The protocol from Bradford (1976) was followed. General esterase activities were determined using the alpha and beta naphtyl acetate substrates (α- and β-NAs). The reaction was conducted for 20 min and stopped with fast blue. Esterases were identified as bands developed by the catalysis of α- and β-NA's as substrates. Based on the results, they were named as α-esterases and β-esterases, respectively [31,32].

Esterase activity for Carbonic anhydrase II (hCA II)

The carbonic anhydrase activity was assayed at 348 nm by following the change of 4-nitrophenylacetate (NPA) to 4-nitrophenylate ion over a period of 80 sec at 25 ^{0}C using spectrophotometer according to the method described in the literature. The substrate was added to 120 µL volume of six different concentrations of inhibitors. Reaction was started by adding of 170 µL of 0.05 M tris-SO_4 buffer (pH: 7.6) and 0.1 µL enzyme solution for a final volume of 300 µL [33, 34].

Determination of IC_{50} values

Esterase activity of carbonic anhydrase II (hCA II) was assayed by the hydrolysis of p-nitro phenyl acetate (PNPA) to p-nitro phenolate (PNP). IC_{50} (the half maximal inhibitory concentration) values of the inhibitors [35] were determined on hCA II isoenzyme. Four different concentrations of compounds (16.6 µM, 8.3 µM, 3.33 µM, 0.033 µM,) as inhibitors and 100 µL of 3 mM *p*-nitro phenyl acetate as substrate were used for enzyme inhibition studies. Reaction was started by addition of 170 µL of 0.05 M tris-SO_4 buffer (pH: 7.6) and 10 µL enzyme solutions. The absorbance was determined at 348 nm after 80 sec. and it was repeated three times for each inhibitor. In order to determine IC_{50} values, percent inhibition graphs were drawn by using statistical packing program on a computer [36, 37].

3. Results and Discussion

3.1. Characterization of compounds

In IR spectra of *ptsmh*, the strong bands observed at 3345 cm^{-1}, 3261 cm^{-1} and 1640 cm^{-1} are assigned to the $\upsilon_{as(NH_2)}$, $\upsilon_{s(NH_2)}$ and $\delta_{(NH_2)}$ modes, respectively. Shifting of $\nu_{(C=N)}$ frequency at 1651 cm^{-1} of *afptsmh* to lower frequency by ~45-51 cm^{-1} (1600–1606 cm^{-1}) and also, $\nu_{(C-O)}$

frequency at 1240 cm^{-1} to higher frequency by ~47-63 cm^{-1} (1287-1303 cm^{-1}) are the evidence of the complexation through imine-N and carbonyl-O with metal ions. This is further confirmed by the appearance of the new band at 555-570 cm^{-1} due to (M-O) stretching modes in the metal complexes. In IR spectra of *afptsmh*, vibrational bands observed at 1268 cm^{-1} and 1089 cm^{-1} are assigned to $\upsilon_{as(SO_2)}$ and $\upsilon_{s(SO_2)}$ stretching modes, respectively. No shifting of symmetric and asymmetric SO_2 modes in the complexes is attributed to nonparticipating in coordination.

3.1.1. Vibrational spectral analysis

Vibrational frequencies and corresponding vibrational assignments of *afptsmh* have been investigated, experimentally and theoretically. Vibrational frequencies of *afptsmh* were calculated at the DFT levels with B3LYP (Becke-Lee-Yang-Parr three parameters) hybrid functional [38]. DFT/B3LYP is the most used method in providing reasonable acceptable vibrational wave numbers for organic molecules. Theoretical calculations were performed using the Gaussian 03W software package. The vibrational band assignments were performed at B3LYP/6-311++G(d,p) theory level combined with scaled quantum mechanics force field (SQMFF) methodology to compare the experimental and calculated vibrational frequencies of molecule. The vibrational modes were assigned on the basis of PED analysis using SQM program [39]. The visual check for the vibrational band assignments were also performed by using Gauss-View program. In order to enable assignment of observed peaks, we evaluated some important characteristic vibrational frequencies of *afptsmh* and compared with experimental values. The calculated vibrational data show good agreement with the experimental results as seen in Table 1.

O-H vibrations

In this study, the experimental O–H stretching vibration was observed at 3376 cm^{-1} and calculated at 3743 cm^{-1} [40]. The largest differences between experimental and theoretical values are evaluated due to the intermolecular hydrogen bonding interactions. We note that our experimental results are belong to solid phase having intermolecular interactions and also, theoretical calculations were performed for isolated molecule in the gaseous phase.

C–H and CH_3 vibrations

The characteristic C–H stretching vibrations of aromatic compounds occur above 3000 cm^{-1} [42-44]. In present study, symmetric C–H stretching vibrations were observed at 3306 cm^{-1} and calculated at 3066 cm^{-1}. Asymmetric C–H stretching vibrations were observed at 3067 cm^{-1} and calculated between 3064-3028 cm^{-1}. The C-H in plane bending vibrations were observed at 1485, 1240, 1157, 1102, 1089 cm^{-1} and calculated at 1432, 1430, 1232, 1154, 1098, 1065 cm^{-1}, respectively. [42,43]. Our molecule has two benzene rings with different chemical environment, C-H vibrations were also observed in the form of doublet pairs as reported in our previous study [50].

The vibration bands at 3004 cm^{-1} and 2917 cm^{-1} correspond to the asymmetric and symmetric stretching of CH_3 groups were calculated in the region 3028-2945 cm^{-1}, as well as at 2897, 2898, 2896 cm^{-1}, respectively (Table 1).

C–C vibrations

Aromatic C–C stretching vibrations, $\nu_{(C-C)}$ occur in 1625-1400 cm^{-1} region with variable intensities. $\nu_{(C-C)}$ bands are observed at 1468-1583, 1625-1590, 1590-1575, 1540-1470, 1460-1430,1380-1280 cm^{-1} as reported by Varsanyi [45]. In this study, $\nu_{(C-C)}$ bands were observed

at 1645, 1586, 1485, 1338 cm^{-1} and calculated at 1620, 1611, 1598, 1592, 1489, 1477, 1432, 1430, 1331 cm^{-1}, respectively.

S=O vibrations

The SO_2 symmetric and asymmetric stretching vibrations occur in the range 1160±30 cm^{-1} and 1330±30 cm^{-1} [46,47]. While the asymmetric SO_2 vibration was observed at 1268 cm^{-1}, the symmetric SO_2 vibration was observed at 1089 cm^{-1}. The asymmetric and symmetric SO_2 vibrations were calculated at 1272 and 1097 cm^{-1}, respectively.

C–S and C–O vibrations

The assignment of C–S stretching vibrations is very difficult for compounds. The C–S stretching vibrations of 3-(4-fluorophenyl)tiophene,3-(4-nitrophenyl)tiophene,3-(4-cyano phenyl)tiophene were observed at 867, 869, 873 cm^{-1} as reported by Mei-Rong [48]. The C–S stretching vibrations of some methanesulfonamides [49] and n-(substituted phenyl)-methanesulfonamide derivatives [50] are also assigned in the region of 789-740 cm^{-1}. In our previous study, $\nu_{(C-S)}$ stretching vibration was observed at 664 cm^{-1} [44]. For our synthesized molecule, the C–S stretching vibration was observed at 671 cm^{-1} and calculated at 650 cm^{-1}, respectively. Similarly, C–O stretching vibration was observed at 841 cm^{-1} and calculated at 823 cm^{-1}, respectiverly.

S–N and C–N vibrations

The S–N stretching vibrations are observed in different frequencies, generally occur between 970-800 cm^{-1} region [47, 50, 51]. In this study, S–N stretching vibrations were observed at 702 cm^{-1} and calculated at 689 cm^{-1}, respectively.

The assignments of C–N stretching vibrations were studied for 1,2-diaminoethane [52-54] and observed between 878-1100 cm^{-1}. In our study, C–N stretching vibration was observed at 1014 cm^{-1}.

3.1.2. NMR spectra

NMR spectra (^{1}H-^{13}C) of *ptsmh* and *afptsmh* were measured and interpreted in $CDCI_3$. In order to facilitate the interpretation of NMR spectra, quantum-chemical calculations were performed using B3LYP/6-311G++(d,p) basis set in $CDCI_3$ phase. Isotropic shielding tensors of ^{13}C NMR were changed into chemical shifts by using linear relationship suggested by Blanco et al. [55]. A similar relationship proposed by Silva et al. [56] was used to obtain chemical shifts for ^{1}H NMR. ^{1}H and ^{13}C NMR spectra of *afptsmh* in $CDCI_3$ were given in Fig. 2. The experimental and calculated chemical shift values were presented in Table 2. In ^{1}H NMR spectra of *ptsmh*, Ar-C**H$_3$** and N-C**H$_3$** proton signals were observed at 2.263 ppm and 3.419 ppm, respectively. The chemical shift belongs to N**H$_2$** was observed at 4.6 ppm as singlet. In ^{1}H NMR spectra of *afptsmh*, Ar-C**H$_3$**, N-C**H$_3$** and N=C-C**H$_3$** protons appeared at 1.292 ppm, 2.198 ppm and 3.780 ppm were calculated at 1.477 ppm, 2.380 ppm and 3.101 ppm, respectively. A signal belong to phenolic O-H proton was observed at δ =10.459 ppm and calculated at 9.465 ppm, respectively. This difference is attributed to existence of intramolecular hydrogen bonding between OH and CN groups. Signals in the range of 6.908-7.351 ppm are belong to aromatic protons. In ^{13}C NMR spectra of *ptsmh*, Ar-**C**H_3 and N-**C**H_3 carbon signals were observed at 20.390 ppm and 33.476 ppm, respectively. ^{13}C-NMR spectra of *afptsmh* were assigned at 18.817 ppm, 27.222 ppm and 39.988 ppm, calculated at 15.2072 ppm, 21.631 ppm and 35.586 ppm for Ar-**C**H_3, N-**C**H_3 and N=C-**C**H_3 groups, respectively. Imine (**C**=N) carbon was observed at 155.210 ppm and also calculated at 174.299 ppm in weak field. Signals in 124.199-155.210 ppm region are belong to aromatic carbons.

3.1.3. Electronic spectra, conductivity and magnetic behavior

The significant electronic spectra of ligand and its complexes were recorded in DMSO between 200-800 nm. The important bands for ligand and its complexes were observed in the region of 290-272 nm and 438-330 nm. Pt^{2+} and Pd^{2+} complexes show two weaker bands at 353-354 nm and 319-335 nm assigned as spin-forbidden d–d transitions. These two bands are attributed to $^1A_{1g} \rightarrow {}^1A_{2g}$ (ν1) and $^1A_{1g} \rightarrow {}^1B_{1g}$ (ν2) transitions [24,57] that indicates a square planar environment around the metal ions. In the electronic spectra of tetrahedral Co(II) complex, three spin-allowed bands are expected for $^4A_2(F) \rightarrow {}^4T_2(F)$, $^4A_2(F) \rightarrow {}^4T1(F)$ and $^4A_2(F) \rightarrow {}^4T_1(P)$ transitions. In general, such complexes show two bands which can be assigned to $^4A_2(F) \rightarrow {}^4T_2(F)$ and $^4A_2(F) \rightarrow {}^4T1(F)$ electronic transitions, $^4A_2(F) \rightarrow {}^4T_1(P)$ is also observed as shoulder. In this study, we couldn't detect $^4A_2(F) \rightarrow {}^4T_2(F)$ transition usually observed out of visible field (over 800 nm), whereas $^4A_2(F) \rightarrow {}^4T1(F)$ transition was observed at 425 nm [58].

The molar conductivities (Λ_m) of metal complexes in DMSO were measured at room temperature. Conductivity results show that metal chelates are non-electrolyte.

The magnetic moments of metal complexes were measured at room temperature. Pd(II) and Pt(II) complexes have diamagnetism as expected, but Co(II) complex has paramagnetism (μ_{eff}=3.89 B.M.) which is correspond to 3 unpaired electrons of high-spin Co(II) complex in Td geometry.

3.1.4. Frontier molecular orbital (FMO)analysis

The FMO calculations indicate that ligand and its complexes have 79 and 167 occupied molecular orbitals, respectively. The energy band gaps between the highest occupied molecular orbital (HOMO) and the lowest unoccupied molecular orbital (LUMO) for mentioned compounds are given in Fig. 3**.** The HOMOs are as electron donors representing

the ability to donate an electron and LUMOs are as electron acceptors representing the ability to obtain an electron. The frontier molecular orbitals (FMOs) play an important role in electronic and optical properties, as well as in UV-vis spectra and chemical reactions [59]. Also, the energy band gap between HOMO and LUMO is a critical parameter in determining molecular electrical transport properties. The electronic system with a larger HOMO-LUMO gap, $\Delta E_{(HOMO-LUMO)}$ should be less reactive than smaller energy gap [60]. The energy values of other HOMO and LUMO levels are listed in Table 2. In this study, FMO energy band gap of *afptsmh* was found to be 4.55 eV obtained by B3LYP method using LanL2DZ basis set. FMO energy band gaps for Co(II), Pd(II) and Pt (II) complexes were also found 1.57 eV, 0.87 eV and 0.41 eV with the same basis set. The energy band gaps of metal complexes are reduced by about 65%, 81% and 90%, respectively.

The LUMO energy describes electrophilicity of the compound and its level has the importance because of the donor-acceptor interaction. Molecule with lower LUMO energy value accepts the electron more easily than higher's and by the way the reactivity of the molecule increases. The lower band gap affects the binding affinities to the biologic molecules, therefore energy gap is one of the most important descriptor for structure-activity relationship. Metal complexes having lower energy gaps show stronger activites than ligand with higher energy gap. Pd(II) complex was found to have the highest activity against CA II enzyme, although Pt(II) complex has the lowest energy gap calculated as 0.41 eV. There is no correlation between biological activitiy and $\Delta E_{(HOMO-LUMO)}$ band gap for metal complexes.

3.2. Antibacterial activities

The compounds were screened in vitro for their antibacterial activities against Gram positive species; *B.subtilis* ATCC 6633, *B. cereus* NRRL-B-3711, *S. aureus* ATCC 6538, *E. faecalis* ATCC 29212, *S. agalactiae* ATCC 13813 and Gram negative species; *E. coli* ATCC 11230,

P. aeruginosa ATCC 15442, *K. pneumonia* ATCC 70063 of bacterial strains by the microdilution (Table 3) and disc diffusion **(**Table 4**)** methods. The activity results were compared with those of the standard drugs; sulfamethoxazole and sulfioxazole **(**Fig. 4**)**.

As seen in antibacterial activity results, the compounds have broad spectrum of activities against tested bacteria at the concentrations of 15.62–2000 µg/mL. *ptsmh* exhibits enhanged inhibition against most of tested bacteria, but *afptsmh* shows the weakest activity against all bacterial strains.

Pd(afptsmh)$_2$ and *Pt(afptsmh)*$_2$ complexes show more activities against *P. aeruginosa* and *Bacillus cereus* at the concentration of 125 µg/mL and 250 µg/mL whereas sulfisoxazole is found less active against bacteria mentioned above. The disc diffusion assay results evidently show that ligand and its complexes have better inhibition activities against *B. subtilis* than sulfamethoxazole and sulfisoxazole. In general, synthesized compounds have higher inhibition effects against Gram positive bacteria than Gram negative bacteria, the antimicrobial activities of the complexes increase in the order of Pd(II)>Pt(II)>Co(II), respectively.

Obtained bacterial results are in accord with similar microbiologic studies for other hydrazones. Previously, Arslan et al. evaluated in vitro antibacterial effect of aroylhydrazones and their Co(II), Ni(II), Cu(II), Pt(II) and Pd(II) complexes against Gram positive bacteria (*S. aureus, B.subtillis, B.cereus, E. feacalis,S. epdermidis*) and Gram negative bacteria (*P. aeruginosa, K. pneumonia, E. coli, P. fluorescens)* using disc diffusion method [57]. Activity results show that *afptsmh* and its Pd(II), Pt(II) complexes have efficiencies up to 18 mm diameter zone against all the test microorganisms. Also, Alyar and Erdem demonstrated that sulfonylhydrazone and its Co(II), Pd(II) complexes possess broad spectrum of activities

against Gram positive bacteria (*S. aureus, B.subtillis, B.cereus, E. feacalis*) and Gram negative bacteria (*P. aeruginosa,K. pneumonia, E. coli)* [24]. Activity results were found between 500-62.5 µg/mL by microdillution method and 11-18 mm by disc diffusion method.

3.3. Carbonic anhydrase II (hCA II) activities

It is well-known that metal complexing anions and sulfonamides bind to human carbonic anhydrase II (hCA II) isoenzyme and represent well investigated classes of inhibitors against this isoenzyme [61]. In our study, we examined the inhibitory actions of sulfonamides on CA II from human by assaying the inhibition of the esterase activity mentioned above. Esterase activities of *afptsmh* and Co(II), Pd(II), Pt(II) complexes at different concentrations are given in Fig. 5. Metal complexes especially *Pd(afptsmh)*$_2$ with IC_{50} value of $2.15x10^{-2}$ mM has higher inhibition effects than *afptsmh* as seen in Table 5. Ozdemir et al. evaluated anticarbonic anhydrase II activities of alkyl sulfonic acide hydrazides. The inhibition results indicate that those compounds have lower activities than our synthesized compounds [22].

General esterase activities were determined using alpha naphtyl acetate (α-NA) and beta naphtyl acetate (β-NA) substrates against *D. Melanogaster Hikone R6.* It was found that *Pd(afptsmh)*$_2$ (1,713nmol α naphthol/min/mg) has the strongest activity against *D. melanogaster* populations for α-NA activity, *ptsmh* (0,891 nmol β-NA/min/mg) and *Pd(afptsmh)*$_2$ (0,731nmol β-NA/min/mg) have higher activities than *afptsmh* (0,595 nmol β-NA/min/mg) towards *D. melanogaster* for β-NA activities as seen in Fig. 6.

Conclusions

Theoretical studies were performed to *afptsmh* using B3LYP/6-311G++(d,p) basis set combined with SQMFF for the vibrational band assignments. Excellent agreement was found between the computed and experimental results in electronic spectra, which was recorded between 290-272 nm, was converted 4.28-4.56 eV and calculated at 4.55 eV. The reaction of Schiff base with metal ions leads to the formation of Schiff base complexes, [ML_2] (where, M:Co(II), Pd(II) and Pt(II)). Diamagnetic Pt(II) and Pd(II) complexes indicate a square planar environment around the metal ions, while Co(II) complex has high spin Td geometry with paramagnetic behavior. FMO (HOMO and LUMO) energies of ligand and metal complexes were calculated using LanL2DZ basis set in B3LYP method. The FMO energy levels are very important parameters in chemical and pharmacological processes giving information on the electron donating and accepting characters of the compounds. The energy band gap between HOMO and LUMO is a critical parameter in determining molecular electrical transport properties. The lower band gap affects the binding affinities to the biologic molecules. FMO energy gaps were found 4.55 eV for *afptsmh* and 0.41-1.57 eV for metal complexes. Metal complexes with lower energy band gaps have stronger antibacterial activites than parent ligand up to MIC's of 62.5 µg/mL in microdillution method and 20 mm zone diameter in disc diffusion method. And also, carbonic anhydrase II (hCA II) inhibition results show that all complexes posses higher biological activities than ligand with increasing order of Pd(II)>Pt(II)>Co(II) and also, it can be mentioned that Pd(II) complex is the strongest hCAII enzyme inhibitor with IC_{50} of $2.15x10^{-2}$ mM.

Acknowledgments:

The authors would like to thank Ahi Evran University BAP (Grant No: FBA-11-30) for the financial support of this project. Authors also thank **Prof. Figen Erkoç** for their valuable

suggestions. I'm thankful to Zafer Bahceci (Zafer Bahceci, died in February 17, 2016) for scientific support.

References

[1] G. Domagk, Deut. Med. Wochenschr. 61 (1935) 250-258.

[2] G.L. Mandell, W.A. Petri, J.G. Hardman, L.E. Limbird, P.B. Molinoff, R.W. Ruddon, A.G. Gilman, Goodman's and Gilman's the Pharmacological Basis of Therapeutics, ninth ed., McGraw-Hill, New York, 1996, pp. 1073–1101.

[3] S. Alyar, H. Alyar, U.O. Ozdemir, O. Sahin, K. Kaya¸ N. Ozbek, A.B. Gündüzalp, J. Mol. Struct. 1094 (2015) 237-245.

[4] T. Nogrady, Medicinal Chemistry, second ed., Oxford University Press, New York, 1988, p. 383.

[5] H.M. Chang, Tsai, S.S. Jung Lee, C. Kunin, P.C.Lin, S.R. Wann, Y.S. Chen, J. Chene. Med. Assoc. 79 (2016) 314-319.

[8] S.M. Kang, K.Y. Nam, S.Y. Jung, K.H. Song, S.K. Kho, K.T. No, H.K. Choi, J.Y. Song, Bioorg. Med. Chem. 26 (2016) 1322-1328.

[9] J.E.F. Reynolds, The Extra Pharmacopoeia, Royal Pharmaceutical Society, London, 1996, pp. 580-581

[10] A. Asraf, W.A. Siddiqui, J. Akbar, G. Mustafa, H. Krautcheid, N. Ullah, B. Mirza, F. Sher, M. Hanif, C.R. Hartinger, Inorg. Chim. Acta 443 (2016) 179-185.

[11] A.A. El-Bindary, A.Z. El-Sonbati, A.F. Shoair, A.S. Mohamed, J Mol. Liquids, 220 (2016) 409-425.

[12] Z. H. Chohan, K. Mahmood-Ul-Hassan Khan, C.T. Supuran, J Enzym. Inhib. Med. Chem. 20 (2005) 183-188.

[13] M. Bragagni, M. Bozdag, F. Carta, A. Scozzafava, C. Lanzi, E Masini, P. Mura, C.T. Supuran, Bioorg. Med. Chem. 23 (2015) 6223-6227.

[14] W. M. Eldehna, M. Fares, M. Ceruso, H.A. Ghabbour, S.M..Abou-Seri, H.A.Abdel-Aziz, D.A.A. Ella, C.T. Supuran, Eur. J Med. Chem. 110 (2016) 259-266.

[15] F. Carta, A.Maresca, A.Scozzafava, C.T. Supuran, Bioorg. Med. Chem. 20 (2012) 2266 2273.

[16] N. Özbek, H. Katırcıoglu, N. Karacan and T. Baykal, Bioorg. Med. Chem. 15 (2007) 5105-5109.

[17] N. Özbek, S. Alyar, H. Alyar, E. Şahin, N. Karacan, Spectrochim. Acta Part A, 108 (2013) 123-132.

[18] Ü.Ö. Özdemir, N. Akkaya, N. Özbek, Inorg. Chim. Acta 400 (2013) 13-19.

[19] S. Alyar, N. Özbek, N. Ocak İskeleli, N. Karacan, Med. Chem. Research. 22 (2013) 2051-2060.

[20] A. Ienco, C. Mealli, P. Paoli, N. Dodoff, Z. Kantarci, N. Karacan, New J. Chem. 23 (1999) 1253-1260.

[21] N. Özbek, S. Alyar, N. Karacan, J. Mo.l Struct. 938 (2009) 48-53.

[22] Ü.Ö. Özdemir, F. Arslan, F. Hamurcu, Spectrochim. Acta Part A 75 (2010) 121-126.

[23] N. Özbek, G. Kavak, Y. Özcan, S. Ide, N. Karacan, J. Mol. Struct. 919 (2009) 154-159.

[24] S. Alyar, S. Adem, Spectrochim. Acta Part A 131 (2014) 294-302.

[25] M.J. Frisch, et al. (2003) Gaussian 03, Revision B.04, Gaussian, Inc., Pittsburgh, PA,

[26] P.C. Hariharan, J.A. Pople, J Chem. Phys. 27 (1974) 209-214.

[27] J.H.B. Nunes, R.E.F. Paiva, A. Cuin, A.M.C. Ferreira, J Mol. Struct. 1112 (2016) 14-20.

[28] A.B. Gündüzalp, N. Özbek, N. Karacan, Med. Chem. Res., 21 (2012) 3435-3444.

[29] P.C. Hariharan, J.A. Pople, J Chem. Phys. 27 (1974) 209-214.

[30] A.W. Bauer, W.M. Kirby, J.C. Sherris, M. Turck, Am. J. Clin. Pathol. 45 (1966) 493-496.

[31] M.M. Bradford, Biochem. 72 (1976) 248-254.

[32] M. Durusoy, N. Diril, A.N. Bozcuk, F.Z. Muluk, Turkish J Zool. 20 (1996) 261-265.

[33] J. McD Armstrong, D.V. Myers, J.A. Verpoorte, J.T. Edsall, J Biol. Chem. 241 (1966) 5137-5149.

[34] S. Bradbury, J. Biol. Chem. 244 (1969) 2002-2009.

[35] İ. Esirden, R. Ulus, B. Aday, M. Tanç, C.T. Supuran, M. Kaya, Bioorg. Med. Chem. 23 (2015) 6573-6580.

[36] Ü.Ö. Özdemir, A. Altuntaş, A. Balaban Gündüzalp, F. Arslan, F. Hamurcu, Spectrochim. Acta Part A, 128 (2014) 452-460.

[37] A.B. Gündüzalp, G. Parlakgümüş, D. Uzun, U.O. Ozdemir, N. Ozbek, M. Sarı, T. Tunç, J Mol. Struct. 1105 (2016) 332-340.

[38] C. Lee, W. Yang, R. G. Parr, Phys. Rev B 37 (1988) 785-789.

[39] SQM version 1.0, Scaled Quantum Mechanical, 2013 GreenAcres Road, Fayetteville, Arkansas 72703

[40] L.A.E. Batista De Carvalho, L.E. Lourenco, M.P.M. Marques, J Mol. Struct. 482–483 (1999) 639-646.

[41] W. Zierkiewicz, D. Michalska, B. C. Matusewicz, M. Rospenk, J Phys. Chem. A 107 (2003) 4547-4554.

[42] R.M. Silverstein, G.C. Bassler, T.C. Morrill, Spectrometric Identification of Organic Compounds, Wiley, New York, 1981.

[43] V. Krishnakumar, R. Ramasamy, Spectrochim. Acta A 62 (2005) 570-577.

[44] H. Alyar, S. Alyar, A. Ünal, N. Özbek, E. Şahin, N. Karacan, J Mol. Struct. 1028 (2012) 116-125.

[45] G. Varsanyi, Assignments of Vibrational Spectra of 700 Benzene Derivatives, Wiley, New York, 1974.

[46] A. Balaban Gündüzalp, Ü. Özdemir Özmen, B.S. Çevrimli, S. Mamaş, S. Çete, Med. Chem. Res. 23 (2014) 3255-3268.

[47] R.M. Silverstein, F.X. Webster, Spectrometric Identification of Organic Compounds.6th ed., Wiley, Asia, 2003.

[48] Y. M. Rong, S. Yu, X. Y. Jin, Springer Plus 3 (2014) 701-713.

[49] Y. Tanaka, Y. Tanaka, Chem. Pharm. Bull. 13 (1965) 858-861.

[50] K.L. Jayalakshmi, B.T. Gowda, Z. Naturforsch. 59a (2004) 491-500.

[51] B.T. Gowda, K. Jyothi, J.J. D'Souza, Z. Naturforsch. 57a (2002) 967-973.

[52] Y.L. Yu, H.H. Huang, J Mol. Struct. 412–420 (1997) 141-152.

[53] S. Kudoh, M. Takayanagi, M. Nakata, T. Ishibashi, M. Tasumi, J Mol. Struct. 479 (1999) 41-52.

[54] L.A.E. Batista De Carvalho, L.E. Lourenco, M.P.M. Marques, J Mol. Struct. 482–483 (1999) 639-646.

[55] F. Blanco, I. Alkorta, J. Elguero, Magn. Reson. Chem. 45 (2007) 797-800.

[56] A.M.S. Silva, R.M.S. Sousa, M.L. Jimeno, F. Blanco, I. Alkorta, J. Elguero, Magn. Reson. Chem. 46 (2008) 859-864.

[57] H.G. Aslan, S. Özcan, N. Karacan, Inorg.Chem. Commuc. 14 (2011) 1550-1553.

[58] R. A. Ahmedi, F. Hasanvand, G. Bruno, H.A. Rudbari, S. Amani, Inorg. Chem. 2013 (2013)1-7.

[59] D.P. Singh, R. Kumar, M. Kamboj, K. Jain, J Coord. Chem. 62 (2009) 2995-3002.

[60] Ç. Yüksektepe, H. Saraçoğlu, N. Çalışkan, İ. Yılmaz, A. Çukurovalı, Bull. Korean Chem. Soc. 31 (2010) 3553-3560.

[61] Ü. Özdemir Özmen, F. İlbiz, A. Balaban Gündüzalp, N. Özbek, Z. Karagöz Genç, F. Hamurcu, S. Tekin, J Mol. Struct. 1100 (2015) 464-474.

Table 1. The vibrational assignments of the *afptsmh* by normal mode analysis based on SQM force field calculations

Exp.	B3LYP/6-31G(d,p)		PotentialEnergyDistributions (P.E.D.)
IR	Unscaledfreq.	Scaledfreq.	Description (%)
3376	3835	3743	υ (OH) (100)
3306	3202	3066	υ_s $(CH)_{ring2}$ (99)
	3202	3066	υ_s $(CH)_{ring1}$ (97)
	3201	3064	υ_{as} $(CH)_{ring1}$ (95)
	3189	3053	υ_{as} $(CH)_{ring2}$ (98)
3067	3175	3040	υ_{as} $(CH)_{ring2}$ (100)
	3169	3033	υ_{as} $(CH)_{ring1}$ (99)
	3164	3028	υ_{as} $(CH)_{ring1}$ (99)
	3157	3022	υ_{as} $(C24\text{-}H_3)$ (100)
	3148	3013	υ_{as} $(CH)_{ring2}$ (99)
3004	3126	2992	υ_{as} $(C20\text{-}H_3)$ (99)
	3108	2975	υ_{as} $(C11\text{-}H_3)$ (100)
	3107	2974	υ_{as} $(C25\text{-}H_3)$ (100)
	3104	2970	υ_{as} $(C20\text{-}H_3)$ (100)
2917	3078	2945	υ_{as} $(C11\text{-}H_3)$ (100)
	3028	2898	υ_s $(C25\text{-}H_3)$ (84) + υ_s $(C20\text{-}H_3)$ (11)
	3027	2897	υ_{as} $(C11\text{-}H_3)$ (100)
	3026	2896	υ_s $(C20\text{-}H_3)$ (83) + υ_s $(C25\text{-}H_3)$ (14)
1651	1662	1650	υ (C24=N) (78) + υ (C24-C25) (5)
1645	1644	1620	υ $(CC)_{ring2}$ (73)
	1636/1613/1523	1611/1592/1477	υ $(CC)_{ring1}$ (70) + δ$(CCH)_{ring1}$ (10)
1586	1620/1528	1598/1489	υ $(CC)_{ring2}$ (73) + δ$(CCH)_{ring2}$ (8)
1563	1495/1488	1446/1440	δ $(C11H_3)$ (91)
1556	1492/1487	1444/1439	δ $(C20H_3)$ (30) + δ $(C25H_3)$ (52)
1485	1478/1475	1432/1430	υ $(CC)_{ring2}$ (27) + υ (C-O39) (5) + δ$(CCH)_{ring2}$ (36) + δ $(C25H_3)$ (5)
1343	1395	1336	υ (C24-C25) (7) + γ $(C25H_3)$ (80)
1338	1355	1331	υ $(CC)_{ring2}$ (75) + δ(COH39) (10)
	1326/1308	1289/1273	υ (C24-C29) (35) + υ (C24-C25) (8) + δ$(CCH)_{ring2}$ (21) + γ (C24C28H28) (11)
1268	1293	1272	υ_{as} (SO_2) (89)
1240	1265	1232	υ (C30-O39) (43) + υ $(CC)_{ring2}$ (23) + δ$(CCH)_{ring2}$ (21)
1157	1195	1154	υ $(CC)_{ring2}$ (12) + δ(CO39-H) (43) + δ$(CCH)_{ring2}$ (21)
	1137	1107	υ $(CC)_{ring1}$ (23) + δ$(CCH)_{ring1}$ (61)
1102	1132	1098	υ $(CC)_{ring2}$ (24) + δ$(CCH)_{ring2}$ (22) + δ(CO39-H) (8) + γ $(C20H_3)$ (8)
1089	1124/1078	1097/1065	υ $(CC)_{ring1}$ (35) + υ_s (SO_2) (22) + υ (CS) (9) + δ$(CCH)_{ring1}$ (8)
	1068	1052	υ $(CC)_{ring2}$ (24) + υ (CN18) (21) + υ (NN) (5) + δ$(CCH)_{ring2}$ (14) + δ $(C25H_3)$ (6)
	1062	1039	γ $(C11H_3)$ (89)
	1060	1033	υ $(CC)_{ring2}$ (36) + υ (CN18) (6) + δ$(CCH)_{ring2}$ (12) + γ $(C25H_3)$ (10)
1014	1053	1025	γ $(C25H_3)$ (80)
	1002	984	υ (C24-C25) (10) + γ $(C25H_3)$ (56)
	993/973/826	981/970/815	γ $(CH)_{ring1}$ (85)
951/900	984/950/760	976/948/759	γ $(CH)_{ring2}$ (87)
865	873	860	υ (NN) (33) + υ (CN18) (8) + δ$(CCH)_{ring2}$ (10)
841	836	823	υ (CO39) (21) + υ $(CC)_{ring2}$ (12) + υ (C24C25) (5) + υ (NN) (6) + δ$(CCC)_{ring2}$ (37)
751	744	738	τ$(CCCH)_{ring2}$ (67)
	721	715	τ$(CCCH)_{ring1}$ (70)
702	699	689	υ (SN) (25) + υ (C24-C29) (8) + υ (C29-C30) (8) + δ$(CCC)_{ring2}$ (7)
671	664	650	υ (CS) (17) + υ (C3-C11) (9) + δ$(CCC)_{ring1}$ (7) + δ$(CCC)_{ring2}$ (6)
654	647	619	δ$(CCC)_{ring1}$ (73)
	637	597	υ (SN) (12) + υ (SC) (5) + δ$(CCC)_{ring2}$ (16) + δ(NC24C25) (5)
	573	563	δ(NC24C29) (5) + δ(NC24C25) (5) + τ$(CCCC)_{ring2}$ (23) + τ$(CCCH)_{ring2}$ (12)
	485	476	δ(SO_2) (10) + δ(OSN) (7) + δ(SNC) (6) + τ(CCSO)(15) + τ$(CCCH)_{ring1}$ (14) + τ$(CCCC)_{ring1}$ (9)
	316	314	τ(CCOH) (67)

ν: bond stretching, δ: in-plane angle bending, γ: out-of-plane angle bending, τ: torsion, as: antisymmetric and s: symmetric.

Table 2. The experimental and theoretical ^{1}H and ^{13}C NMR chemical shifts *δ(ppm)* for *afptsmh*

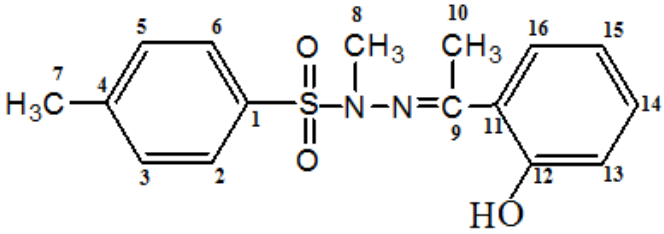

	B3LYP/6-311++G(d,p)[a]	
Assignment	***δ(exp.)***	***δ(calc.)***
C-1	138.888	139.404
C-2	135.204	129.358
C-3	136.842	128.373
C-4	151.002	147.006
C-5	136.842	130.162
C-6	135.204	128.874
C-7	18.817	15.2072
C-8	27.222	21.631
C-10	39.988	35.586
C-9	163.101	174.299
C-11	126.438	127.231
C-12	155.210	155.271
C-13	124.554	114.461
C-14	133.029	131.182
C-15	124.199	120.425
C-16	134.950	132.101
H-2	7.742	7.851
H-3	7.312	7.423
H-5	7.219	7.521
H-6	7.762	7.809
H-7(CH_3)$_{Ar}$	1.292	1.477
H-8$_{(CH3-N)}$	2.198	2.380
H-9	3.780	3.101
H-13	6.929	6.707
H-14	7.351	7.270
H-15	6.908	7.122
H-16	7.330	7.498
OH	10.459	9.465

σ Transform into using equations given in Ref. [55,56]; $\delta^{13}C = 175.7–0.963\ \sigma^{13}C$ and $\delta^{1}H = 31.0–0.970\ \sigma^{1}H$.

Table3. The MICs of antibacterial activity of the compounds

Bacteria strains	***MIC*** *µg/mL* **(mM)**						
Gram- negative	***ptsmh***	***afptsmh***	***Pt(afptsmh)***	***Pd(afptsmh)***	***Co(afptsmh)$_2$***	**SD1**	**SD2**
Eschericha coli ATCC 11230	250 **(1.24)**	500 **(1.57)**	250 **(0.301)**	250 **(0.337)**	500 **(0.720)**	64 **(0.25)**	23.4 **(0.088)**
*Pseudomonas aeruginosa*ATCC 15	250 **(1.24)**	500 **(1.57)**	250 **(0.301)**	125 **(0.168)**	125 **(0.180)**	64 **(0.25)**	375 **(1.403)**
Klebsiella pneumonia ATCC 70063	125 **(0.62)**	250 **(0.78)**	125 **0.150)**	500 **(0.674)**	250 **(0.360)**	16 **(0.063)**	23.4 **(0.088)**
Gram -positive							
Bacillus subtilis ATCC 6633	250 **(1.24)**	250 **(0.78)**	62.5 **(0.075)**	250 **(0.337)**	62.5 **(0.090)**	1500 **(5.92)**	-
Bacillus cereus NRRL-B-3711	250 **(1.24)**	500 **(1.57)**	250 **(0.301)**	125 **(0.168)**	62.5 **(0.090)**	16 **(0.063)**	375 **(1,403)**
*Staphylococcus aureus*ATCC 6538	500 **(2.48)**	500 **(1.57)**	250 **(0.301)**	250 **(0.337)**	62.5 **(0.090)**	32 **(0.126)**	93.75 **(0.35)**
*Enterococcus faecalis*ATCC 29212	500 **(2.48)**	250 **(0.78)**	250 **(0.301)**	250 **(0.337)**	250 **(0.360)**	32 **(0.126)**	93.75 **(0.35)**
*Strepococcusagalactiae*ATCC 1381	15.62 **(0.078)**	125 **(0.39)**	31.25 **(0.0376)**	125 **(0.168)**	125 **(0.180)**	16 **(0.063)**	11.7 **(0.044)**

Table 4. Measured inhibition zone diameter (mm) of the compounds and antibiotics by disc diffusion method

Bacteria strains	***Diameter inhibition zone (mm,200 µg/disk)***						
Gram- negative	***ptsmh***	***afptsmh***	***Pt(afptsmh)$_2$***	***Pd(afptsmh)$_2$***	***Co(afptsmh)$_2$***	***SD1***	**SD2**
Eschericha coli ATCC 11230	13	12	14	14	14	17	20
*P.aeruginosa*ATCC 15442	13	11	13	17	16	17	8
Klebsiella pneumonia ATCC 70063	18	15	16	13	11	24	28
Gram -positive							
Bacillus subtilis ATCC 6633	13	12	16	14	16	-	-
Bacillus cereus NRRL-B-3711	15	13	14	16	17	28	17
*Staphylococcus aureus*ATCC 6538	13	13	15	16	18	15	25
*Enterococcus faecalis*ATCC 29212	14	13	14	16	12	15	18
*Strepococcusagalactiae*ATCC 13813	23	15	17	14	14	23	21

Table5. Inhibitor effects of compounds for the esterase andhydratase activities of human hCA-II

Compounds	IC_{50} mM(Esteraseactivity) hCA-II
ptsmh	$5.15*10^{-2}$
afptsmh	$4.26*10^{-2}$
Pt(a*fptsmh*)$_2$	$3.0*10^{-2}$
Pd(a*fptsmh*)$_2$	$2.54*10^{-2}$
Co(a*fptsmh*)$_2$	$3.56*10^{-2}$
Acetazolamide	$2.15*10^{-2}$

Figure Captions

Fig. 1. (a) The molecular structure of *afptsmh* with the atom-numbering scheme (b) The structure sketches of the complexes

Fig. 2. (a) ^{1}H NMR of the *afptsmh*, (b) ^{13}C NMR of the *afptsmh*

Fig. 3. (a), (b) and (c) Plots of the frontier orbitals of *Co(afptsmh)$_2$, Pd(afptsmh)$_2$, Pt(afptsmh)$_2$* complex **(**d) *afptsmh* and (e) *ptsmh* ligand molecules, respectively.

Fig. 4. (a) Comparison of antibacterial activite, (b) Percentage of inhibition of ligands, metal (II) complexes and antibiotics

Fig. 5. Effect of ligands and metal (II) complexes.at different concentrations on esterase activity of hCA-II

Fig. 6. Mean of total esterase enzyme activities (a) (using α-naphytl acetate as substrate), (b) activities (using β-naphtyl acetate as substrate) of *Drosophila melanogaster* populations

Figure 1

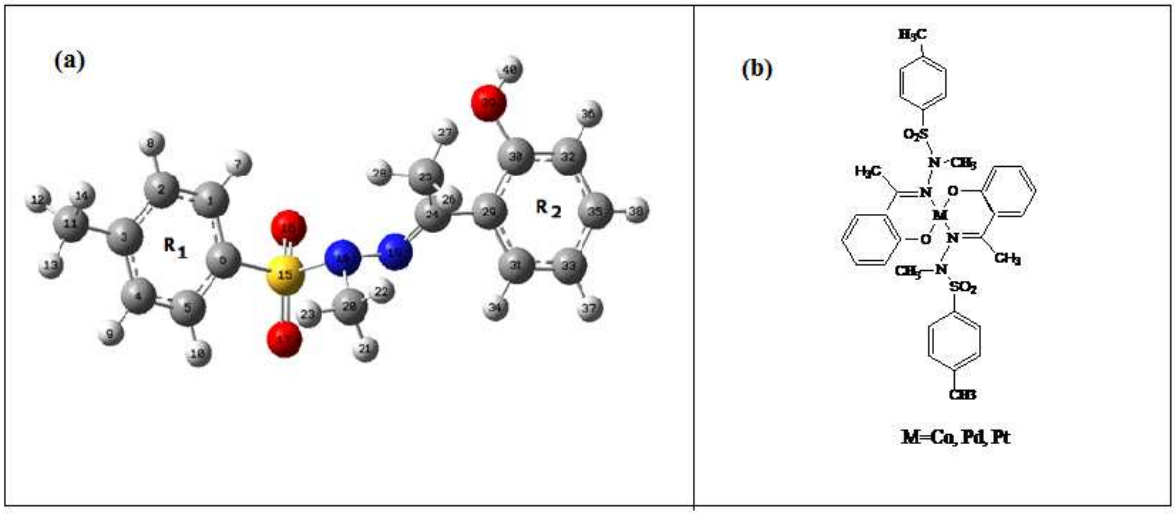

Figure 2

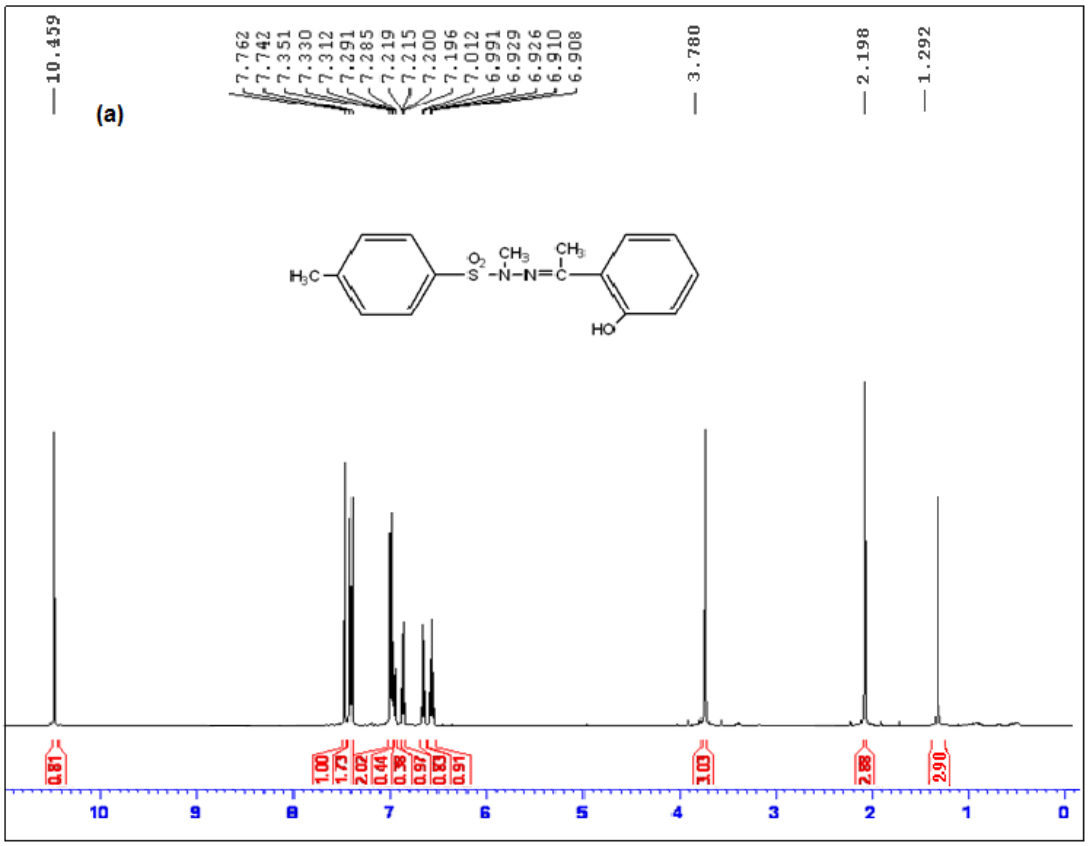
(a)
10.459
7.762
7.742
7.351
7.330
7.312
7.291
7.285
7.219
7.215
7.200
7.196
7.012
6.991
6.929
6.926
6.910
6.908
3.780
2.198
1.292
HO

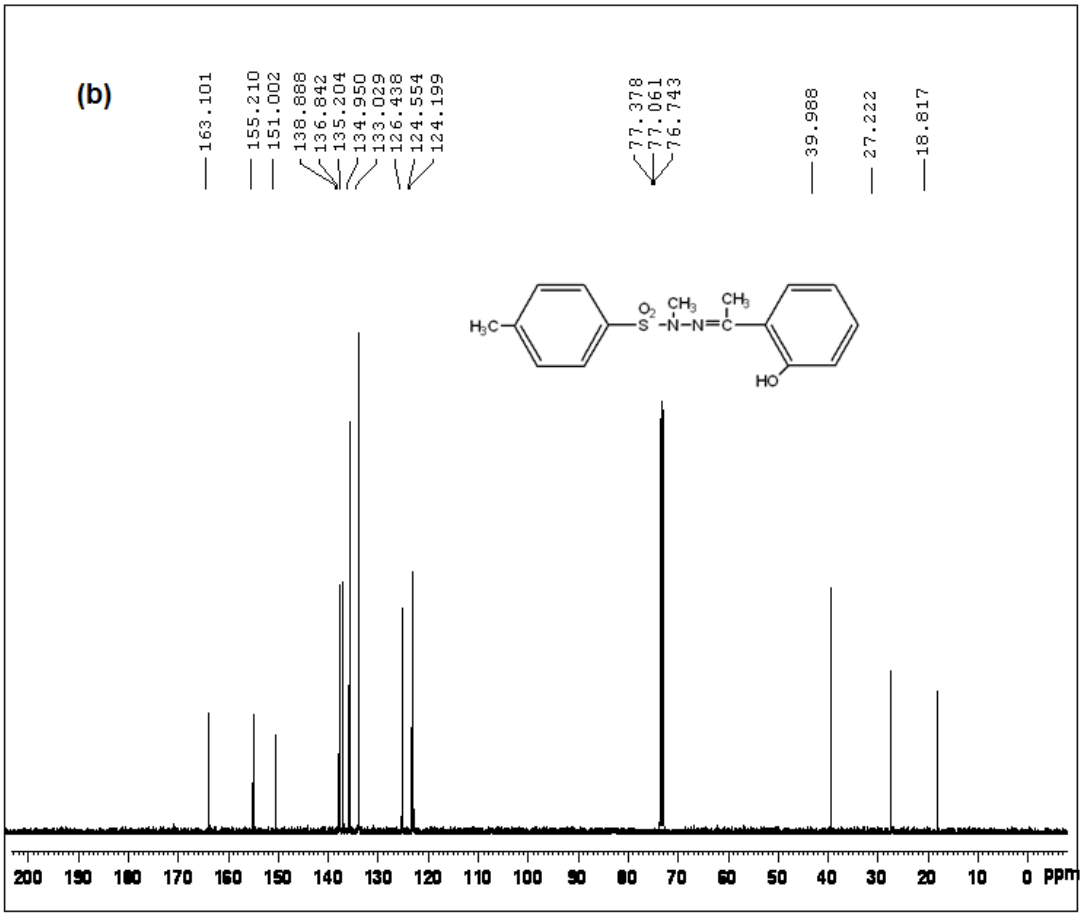
(b)
163.101
155.210
151.002
138.888
136.842
135.204
134.950
133.029
126.438
124.554
124.199
77.378
77.061
76.743
39.988
27.222
18.817
HO
ppm

Figure 3

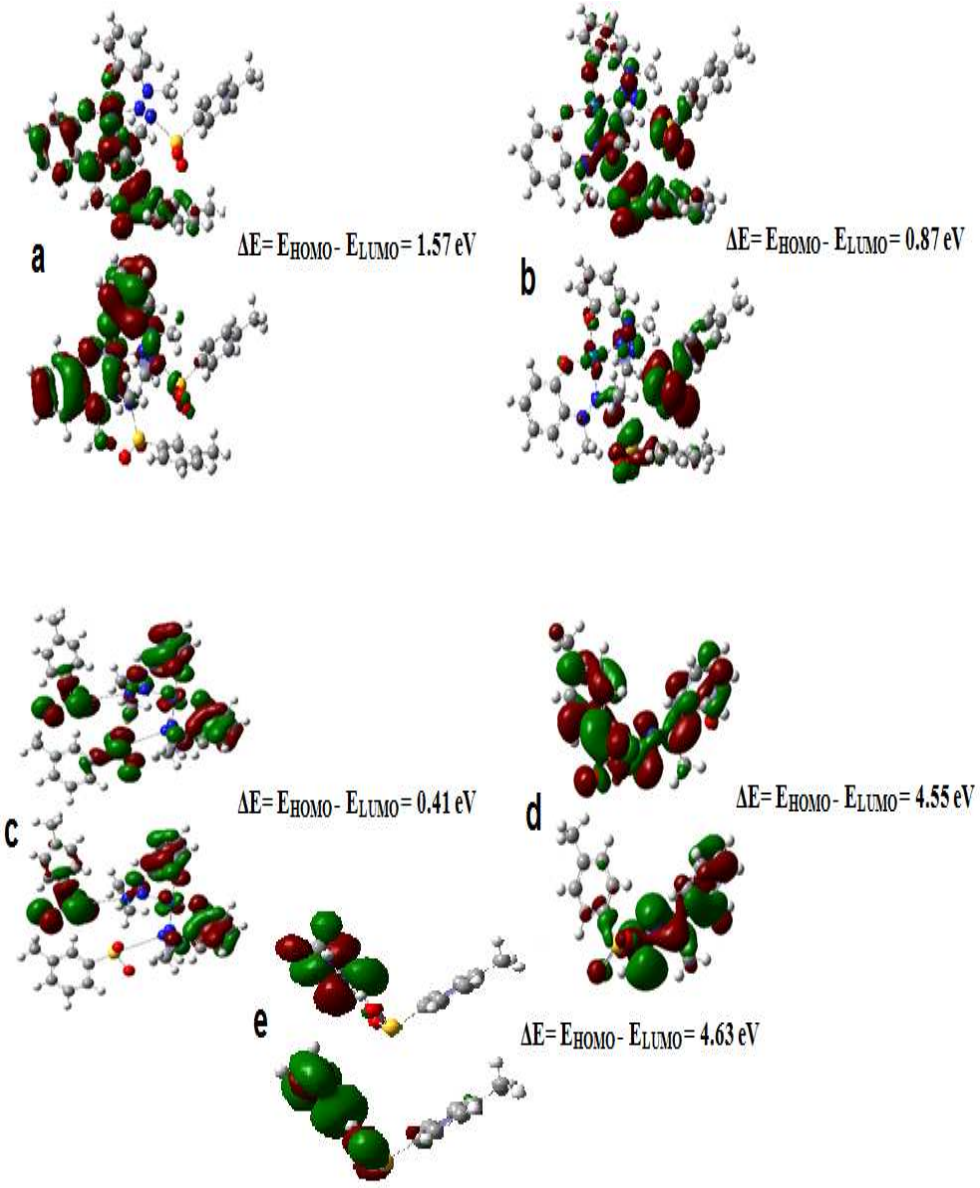
a
ΔE= E_HOMO - E_LUMO = 1.57 eV
b
ΔE= E_HOMO - E_LUMO = 0.87 eV
c
ΔE= E_HOMO - E_LUMO = 0.41 eV
d
ΔE= E_HOMO - E_LUMO = 4.55 eV
e
ΔE= E_HOMO - E_LUMO = 4.63 eV

Figure 4

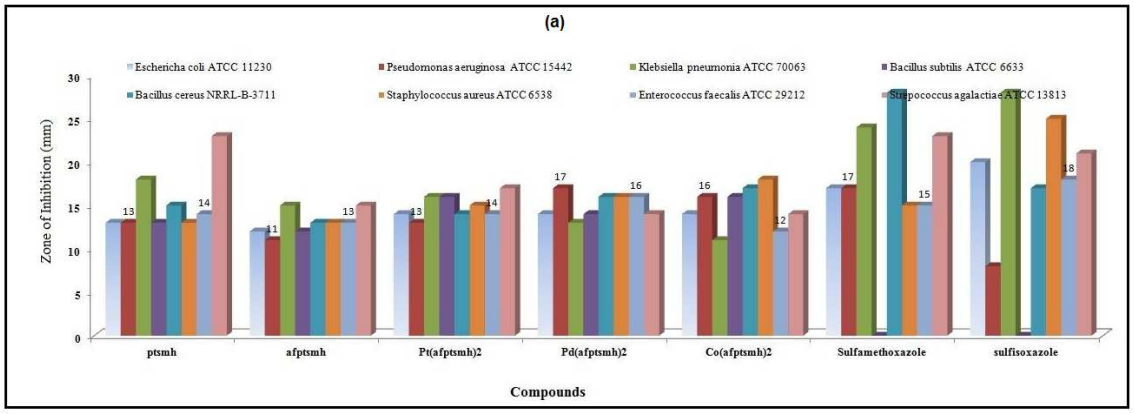

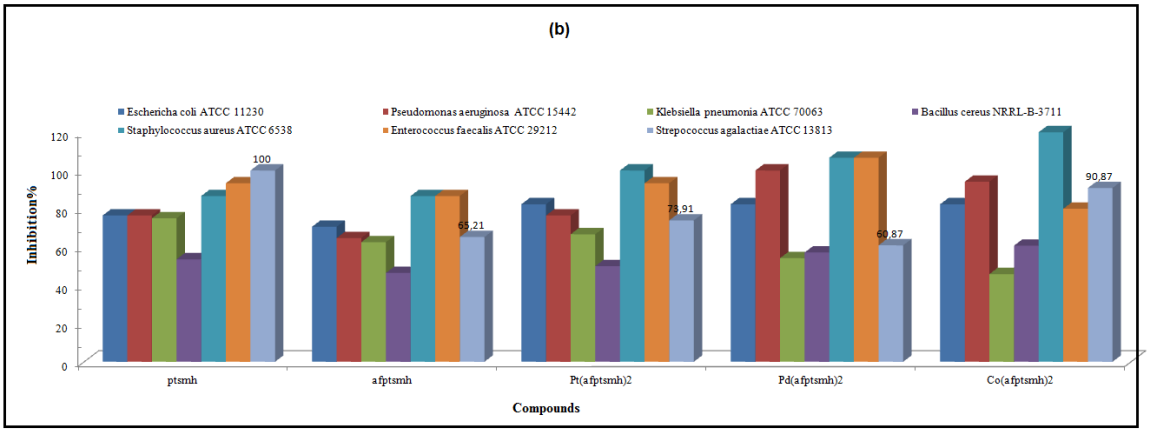

Figure 5

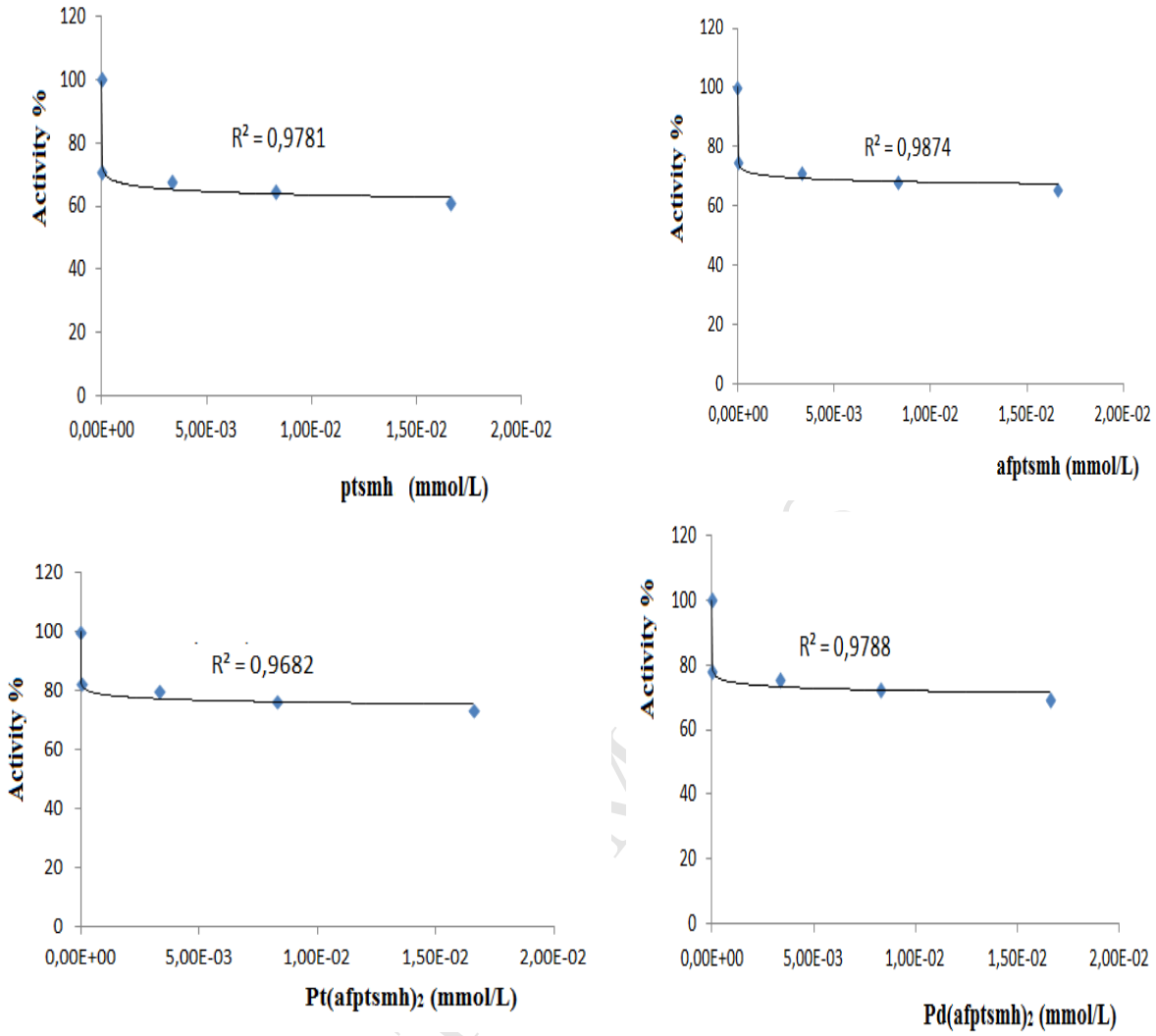
Activity %
R² = 0,9781
ptsmh (mmol/L)
R² = 0,9874
afptsmh (mmol/L)
R² = 0,9682
Pt(afptsmh)₂ (mmol/L)
R² = 0,9788
Pd(afptsmh)₂ (mmol/L)

Figure 6

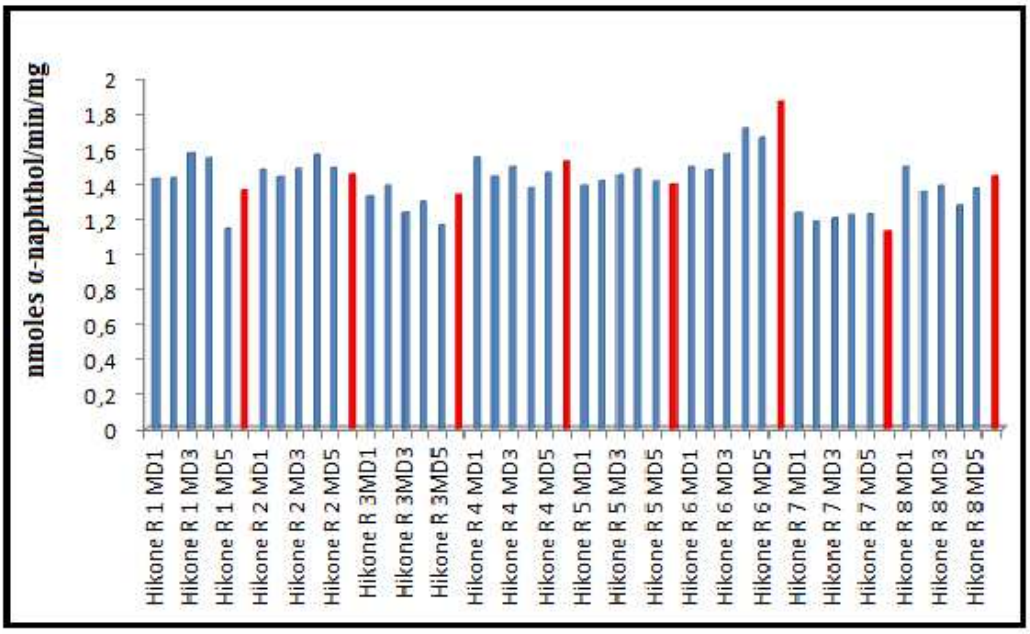
nmoles α-naphthol/min/mg
2
1,8
1,6
1,4
1,2
1
0,8
0,6
0,4
0,2
0
Hikone R 1 MD1
Hikone R 1 MD3
Hikone R 1 MD5
Hikone R 2 MD1
Hikone R 2 MD3
Hikone R 2 MD5
Hikone R 3MD1
Hikone R 3MD3
Hikone R 3MD5
Hikone R 4 MD1
Hikone R 4 MD3
Hikone R 4 MD5
Hikone R 5 MD1
Hikone R 5 MD3
Hikone R 5 MD5
Hikone R 6 MD1
Hikone R 6 MD3
Hikone R 6 MD5
Hikone R 7 MD1
Hikone R 7 MD3
Hikone R 7 MD5
Hikone R 8 MD1
Hikone R 8 MD3
Hikone R 8 MD5

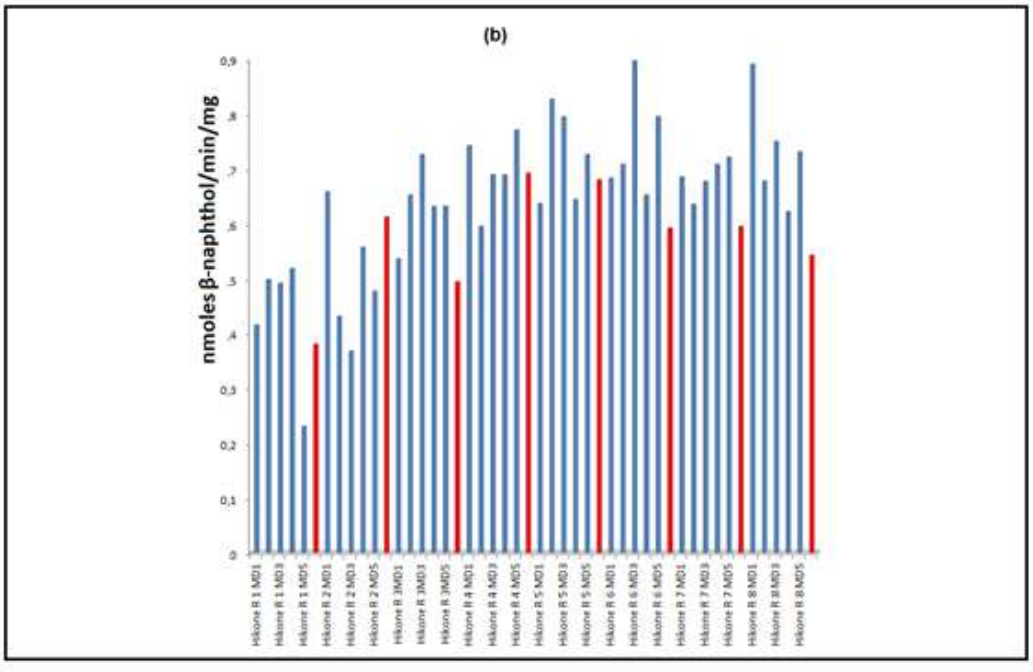
(b)
nmoles β-naphthol/min/mg

Highlights

1. Synthesis of 2-Hydroxyacetophenone-N-methyl p-toluenesulfonylhydrazone *(afptsmh)*
2. Synthesis of *Co(afptsmh)$_2$*, *Pd(afptsmh)$_2$* and *Pt(afptsmh)$_2$* complexes
3. Experimental characterization of afptsmh and its metal complexes
4. DFT computations of afptsmh and its metal complexes
5. Antimicrobial activities of the afptsmh and its Co(II), Pt(II) and Pd(II) complexes
6. Carbonic anhydrase enzyme inhibitor effects of compounds